Minimalist Low-Power Batteryless Temperature Sensor Tag for Non-Invasive Long-Distance Wireless Continuous Monitoring

Andres Seré, Leonardo Steinfeld, Simon Hemour, Pablo Perez-Nicoli

Minimalist Low-Power Batteryless Temperature Sensor Tag for Non-Invasive Long-Distance Wireless Continuous Monitoring

Andrés Sere[#1], Leonardo Steinfeld[#2], Simon Hemour[$3], Pablo Pérez-Nicoli[#$4]

[#]Facultad de Ingeniería, Universidad de la República. Montevideo, Uruguay

[$]IMS Laboratory, University of Bordeaux, Bordeaux, France

{[1]asere, [2]leo, [4]pablop}@fing.edu.uy, [3]simon.hemour@u-bordeaux.fr

***Abstract* — This paper presents a novel and straightforward architecture for a batteryless sensor tag. The tag consists solely of a 25x25 mm spiral antenna used for both wireless power transfer and back telemetry (at 13.56 MHz), along with capacitors, diodes, a transistor, and a transducer element. Due to its operation at high frequency (HF), the proposed system can be used in applications where the surroundings exhibit significant absorption hindering the use of UHF tags. The proposed proof-of-concept prototype employs a thermistor as the transducer element, enabling temperature sensing in a range of -5 to 45 degrees Celsius, achieving reading distances of up to 60 cm.**

***Keywords* — temperature sensors, wireless power transfer, wireless passive sensor, wireless monitoring, batteryless system, resistive sensor, tunnel diode.**

I. Introduction

Wireless sensor networks (WSN) are widely utilized across diverse applications, including precision agriculture, industrial automation, and digital health. The development of batteryless devices is crucial because it enables sensor miniaturization and extends their lifespan, overcoming the limitations imposed by battery durability. These batteryless sensors are usually energized and read wirelessly from a reader device that is either battery-powered or mains-powered.

One of the most frequently monitored physical variables by batteryless WSNs is temperature, used, for instance, to monitor food cold chains [1], [2], bee colony health [3], animal control [4], [5], human health monitoring [6]–[11], among other applications. However, in most cases, and as is also the case with this paper, the same architectures used in these sensors to sense temperature could be repurposed to sense another variable simply by changing the transducer element.

Batteryless sensors can be divided into two main groups: those that use ultra high frequency (UHF) [6], [12], [13] and achieve longer reading distances (up to some meters), and those that use lower frequencies [2], [4], [7]–[11], [14], [15], primarily designed for short distances (a few centimeters). Some studies, such as [5], propose combined systems where HF is utilized to transmit power to the sensor, while UHF is employed for reading.

With regards to high-frequency systems, a reading distance of 20 cm is achieved in [6], [13], but longer distances can also be attained, such as in [12], where a one-meter read distance was reported. One of the main drawbacks of these UHF systems is that within this frequency range, absorption and reflection are not negligible, making their use in certain environments more complex or even unfeasible. For instance, when aiming to communicate with a sensor implanted in a body, buried beneath moist soil, or to sense within a beehive containing substantial honey quantities, employing UHF poses numerous challenges. In such scenarios, the majority of studies opt for lower operating frequencies.

Among batteryless sensors operating at frequencies lower than UHF, the most widely used in recent years have been those operating at 13.56 MHz (HF) [2], [7]–[9], [14] due to the widespread adoption of Near Field Communication (NFC) standards and because this frequency belongs to the industrial, scientific, and medical (ISM) band, with worldwide availability. For these reasons, 13.56 MHz will also be the operating frequency used in this work.

A few minimalist architectures have been proposed [8], [10], [11], [14] which solely rely on a temperature-sensitive resistive element. This element's variation is then detected by measuring the change in impedance reflected back to the energy transmitter (the reader). We will refer to this approach as the analog reflected impedance method. The issue with these architectures is that they only function at distances of a few centimeters, as at greater distances, the variation in the reader's load impedance due to the sensor change is imperceptible. Additionally, this impedance variation must be measured with a dedicated reader, and it is not compatible with commercial standards as NFC. Another approach to batteryless temperature sensors involves utilizing the NFC standard, which requires a complex circuit in the tag [2], [7], [9]. While the NFC standard is typically used for short distances, as seen in [2], [9] (less than 3 cm), [7] reports a system that achieves reading distances of up to 45 cm with the aim of reading wearable sensors from beneath a mattress. There are other examples in the literature where complex sensors are proposed, such as the one presented in [15], which operates at 200 MHz (VHF) and has an 8 mm reading distance. This system utilizes an ASIC that includes rectification, voltage regulation, and all the required logic to implement back telemetry communication.

In this paper, we propose a minimalist batteryless temperature sensor, composed solely of a spiral WPT receiver coil, capacitors, diodes, a transistor, and an NTC thermistor.

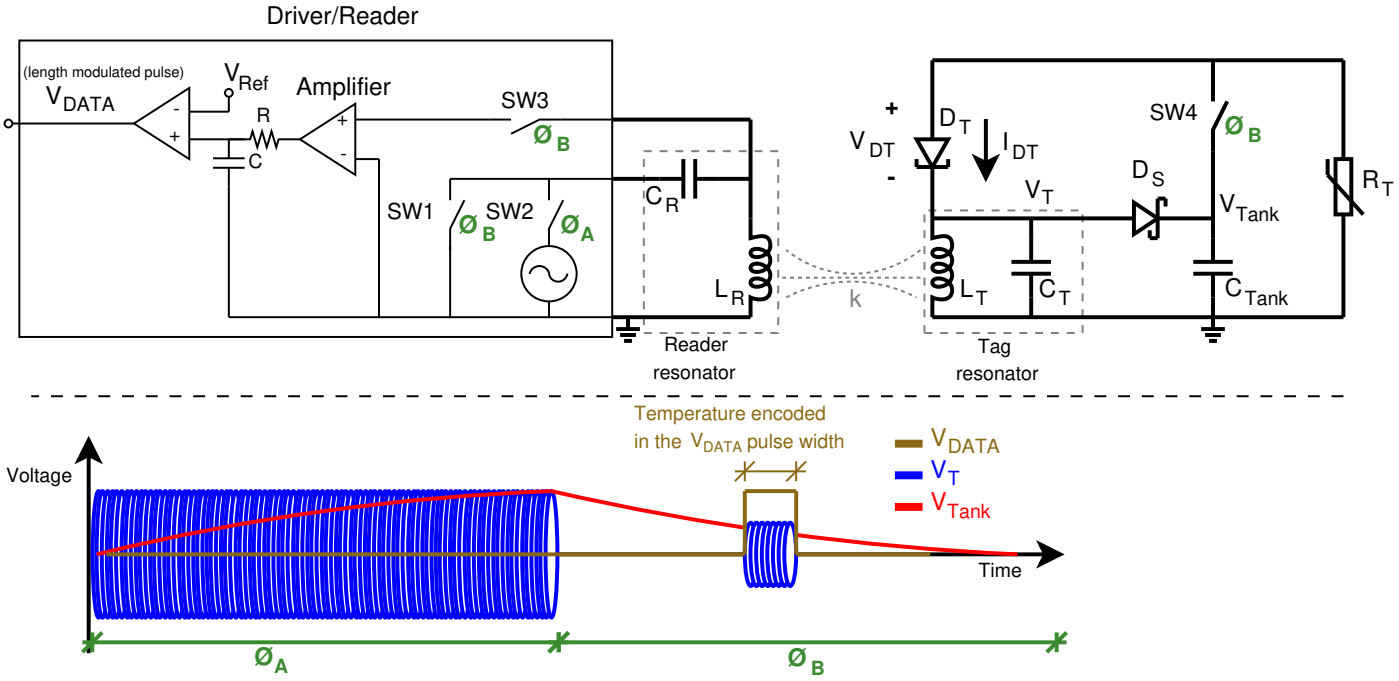

Fig. 1. Block Diagram of the proposed sensor tag and its reader.

Using only these components, we construct a sensor tag capable of energizing and responding up to 60 cm in simulations, a result that is more than competitive with the state of the art. We use a frequency of 13.56 MHz, enabling the use of this sensor in applications where there are absorbent aqueous media, as in implantable or wearable applications, beehive monitoring, or reading sensors buried under moist soil, among many other applications where the use of UHF poses challenges. Although the prototype in this study implements a temperature sensor, the same architecture could be used to sense other variables by changing the transducer utilized. This paper is structured as follows: Firstly, the main concept behind the architecture is introduced in Section II-A. Subsequently, the circuit implementation is described in Section II-B. Simulation results are presented in Section III, followed by the main conclusions in Section IV.

II. Proposed Sensor Tag

A. Main Idea

A block diagram of the proposed sensor is depicted in Fig. 1 and described below. The tag reading process involves two phases: one for energizing the tag (ϕ_A) by the reader, and another for reading/response (ϕ_B), during which the tag transmits the sensed temperature to the reader. This two-phase operation is known as half duplex and is utilized in RFID systems like cattle identification [16], [17]. During phase A, an alternating current at the carrier frequency (13.56 MHz) is generated in the reader coil by a driving circuit. The induced voltage in the coupled tag resonator (L_T-C_T) is rectified to store the received power in a tank capacitor (C_{Tank}). Then, during ϕ_B, the tank capacitor is discharged through a thermistor (R_T) and a tunnel diode (D_T). Hence, the discharge rate will depend on the temperature of the tag. As the discharge progresses, the tunnel diode bias voltage is swept, causing an oscillation to occur in the L_T-C_T tag resonator (at its resonant frequency, 13.56 MHz) within the range that fulfills the oscillation condition as explained later. As a result an oscillating signal is generated in the tag for a duration that encodes the tag's temperature. During this phase (ϕ_B), the reader senses the induced voltage on its resonator (L_R-C_R) to detect the width of the response pulse, thereby completing the reading process.

To conclude the explanation of the architecture proposed, we delve into the oscillation condition of the tunnel diode and how its oscillation time encodes the tag's temperature. The current-voltage (I_{DT}-V_{DT}) curve for a tunnel diode is represented in Fig. 2a. The circuit composed of the tunnel diode and the tag resonator (L_T-C_T) will oscillate when the diode is biased with a voltage V_{DT} in the negative slope region (between the peak V_P and the valley V_V voltages) [18], [19]. This oscillation condition will occur for a certain period of time while the C_{Tank} discharges, as illustrated in Fig. 2b. Since the decay time of V_{Tank} depends on the temperature,

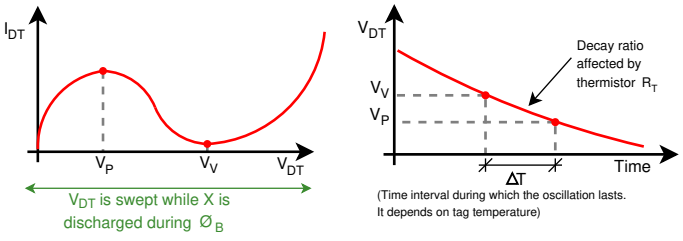

Fig. 2. Tunnel diode oscillator and its temperature encoding in the pulse width: (a) I_{DT}-V_{DT} curve; (b) Bias sweep during C_{Tank} discharge.

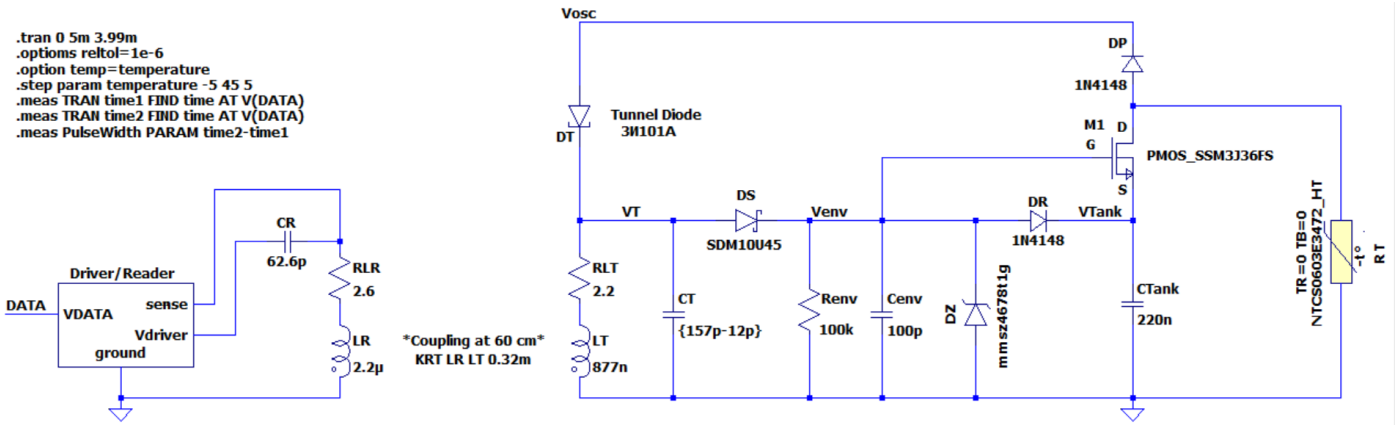

Fig. 3. Schematic of proposed bateryless sensor tag.

as it discharges through the thermistor R_T, the duration for which the diode is biased in the oscillation zone will also depend on the tag's temperature. This achieves an oscillation at the resonance frequency, whose duration encodes the tag's temperature.

In the next section II-B, the circuit implementation is described in detail, including the circuitry required to implement the logic controlling SW3 in the tag.

B. Proposed Circuit

The schematic diagram of the proposed circuit is shown in Fig. 3, detailing the values and part numbers of each component. The additional components, in comparison to those shown in Fig. 1, are necessary for implementing the autonomous control logic of $SW4$, as explained below. The first block, consisting of the Schottky diode DS, resistor $Renv$, and capacitor $Cenv$, implements an envelope detector for the received signal VT. This signal is used to control the $SW4$, which is implemented by transistor $M1$. During phase A (ϕ_A), the tank capacitor is charged from node $Venv$. As phase B (ϕ_B) begins and the reader stops sending the power-up signal, there will be no received signal at VT, causing the envelope signal $Venv$ to drop to zero, turning ON the PMOS transistor $M1$. This will initiate the discharge of $CTank$ through the thermistor RT and the tunnel diode DT, as was explained in the section II-A. The diode added in series with the tunnel diode (DP) is a protection diode to prevent a high reverse voltage from occurring across the tunnel diode, which could damage it. The zener diode (DZ, $V_Z = 1.8$ V) was also included for protection, limiting the voltages on the tag when it is in close proximity to the reader.

The thermistor (RT) was selected to have a current consumption comparable to that of the tunnel oscillator, thus maximizing its influence on the duration of the oscillation ($CTank$ discharge rate). Regarding the tag resonance, the resonant capacitor (CT) ideally should be 157 pF to achieve resonance at 13.56 MHz with the tag coil (LT). However, its value was adjusted to take into account the parasitic capacitance of the other components in the tag, resulting in $CT = 145$ pF. The inductance and equivalent series resistance (ESR) values of the coils used for both the reader (LR, RLR) and the tag (LT, RLT) correspond to measured values of actual coils, which are shown in Fig. 4 and were reported in [20]. The current imposed on the reader coil L_R meets the safety requirements for human exposure, as analyzed in [20].

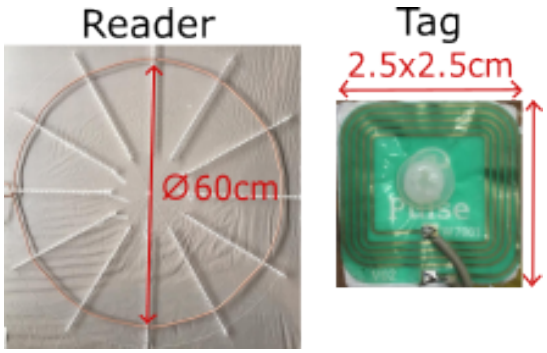

Fig. 4. Reader and Tag coils used in simulations.

III. Simulation Results

Firstly, to showcase the intended operation of the proposed tag, Fig. 5 presents simulation results of various signals during the transition from phase A (ϕ_A) to phase B (ϕ_B). The signal names depicted correspond to the labels shown in Fig. 3.

The first thing we observe at the beginning of the time axis is the last part of ϕ_A, where the signal received at the tag's antenna (VT) is being rectified, and the tank capacitor is already charged. At the end of ϕ_A, i.e. when VT extinguishes, the envelope signal ($Venv$) drops, activating transistor $M1$, initiating the discharge of $CTank$. There is no oscillation during the first $CTank$ discharging phase as it biases the tunnel diode at voltages higher than V_V (Fig. 2a). Once the bias voltage goes down and the negative slope region is reached on the tunnel diode (between V_P and V_V, Fig. 2a), oscillation is generated. Figure 6 plots the pulse width sensed from the reader for different temperatures, demonstrating the feasibility of deducing the tag's temperature from the reader. The simulations shown in both Fig. 5 and Fig. 6 were conducted at a distance of 60 cm between the reader and the receiver, corresponding to a coupling of $k = 0.32$ m.

The proposed system is compared with the state of the art in Table 1.

Table 1. Comparison with the state of the art.

	[12]	[13]	[15]	[11]	[8], [14]	[2], [9]	[7]	This work
Carrier frequency	1.5 GHz	478.5 MHz	200 MHz	27 MHz	13.56 MHz	13.56 MHz	13.56 MHz	13.56 MHz
Back telemetry	Harmonic backscattering	FM parametric oscillation	LSK	Analog reflected impedance	Analog reflected impedance	NFC standard	NFC standard	PWM
Circuit complexity	Low	Low	High (ASIC)	Low	Low	High	High	Low
Distance range	1 m	20 cm	8 mm	20 mm	< 40 mm	< 25 mm	45 cm	60 cm

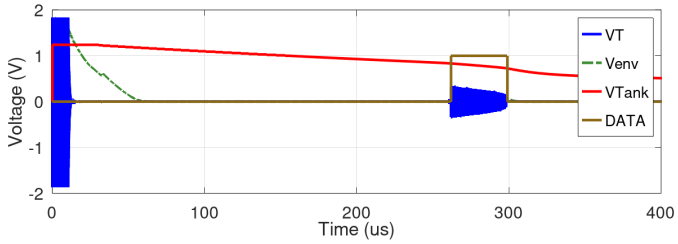

Fig. 5. Simulation results showing the expected operation of the proposed architecture.

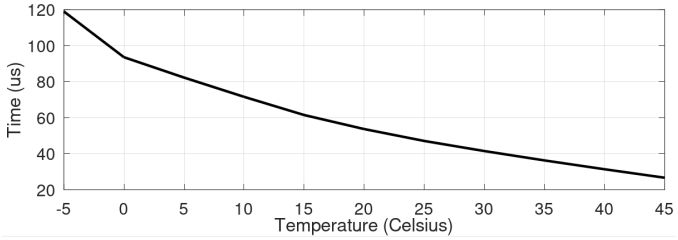

Fig. 6. Pulse width of DATA signal in the reader (Fig.3) as a function of the tag temperature. Simulation conducted at a distance of 60 cm between reader and tag.

IV. Conclusion

This paper demonstrates the feasibility of implementing a simple architecture for a batteryless sensor tag that achieves long distances (up to 60 cm) operating at 13.56 MHz. The use of the tunnel diode allowed harnessing the tag resonator to generate an oscillation from a low voltage, enabling a straightforward circuit design. A simple envelope detector with a transistor was sufficient to detect the end of the tag's energization phase and initiate its response. Although a thermistor was used as the transducer element, it could be replaced by another element whose resistance varies with a different variable of interest.

References

[1] E. Nogues, N. Mackowiack, A. Hamdoun, and M. Latrach, "NFC/RFID sensor tag for wireless temperature monitoring in a cold chain," in *10th International Conference on Innovation, Modern Applied Science & Environmental Studies (ICIES'2022)*, vol. 351, 2022, p. 01 038.

[2] X. Xiao, B. Mu, G. Cao, Y. Yang, and M. Wang, "Flexible battery-free wireless electronic system for food monitoring," *Journal of Science: Advanced Materials and Devices*, vol. 7, no. 2, p. 100 430, 2022.

[3] W. G. Meikle, M. Weiss, P. W. Maes, *et al.*, "Internal hive temperature as a means of monitoring honey bee colony health in a migratory beekeeping operation before and during winter," *Apidologie*, vol. 48, no. 5, pp. 666–680, 2017.

[4] K. Opasjumruskit, T. Thanthipwan, O. Sathusen, *et al.*, "Self-powered wireless temperature sensors exploit RFID technology," *IEEE Pervasive computing*, vol. 5, no. 1, pp. 54–61, 2006.

[5] N. Chaimanonart and D. J. Young, "A wireless batteryless in vivo ekg and core body temperature sensing microsystem with 60 Hz suppression technique for untethered genetically engineered mice real-time monitoring," in *2009 Annual International Conference of the IEEE Engineering in Medicine and Biology Society*, IEEE, 2009, pp. 4872–4875.

[6] F. Camera, C. Miozzi, F. Amato, C. Occhiuzzi, and G. Marrocco, "Experimental assessment of wireless monitoring of axilla temperature by means of epidermal battery-less RFID sensors," *IEEE Sensors Letters*, vol. 4, no. 11, pp. 1–4, 2020.

[7] Y. S. Oh, J.-H. Kim, Z. Xie, *et al.*, "Battery-free, wireless soft sensors for continuous multi-site measurements of pressure and temperature from patients at risk for pressure injuries," *Nature communications*, vol. 12, no. 1, p. 5008, 2021.

[8] S. Consul-Pacareu and B. I. Morshed, "Design and analysis of a novel wireless resistive analog passive sensor technique," *IET Wireless Sensor Systems*, vol. 8, no. 2, pp. 45–51, 2018.

[9] P. Escobedo, M. Bhattacharjee, F. Nikbakhtnasrabadi, and R. Dahiya, "Smart bandage with wireless strain and temperature sensors and batteryless NFC tag," *IEEE Internet of Things Journal*, vol. 8, no. 6, pp. 5093–5100, 2020.

[10] L. Rauter, J. Zikulnig, T. Moldaschl, *et al.*, "Printed wireless battery-free sensor tag for health monitoring of polymer composites," *IEEE Journal on Flexible Electronics*, 2023.

[11] S. S. Karipott, P. M. Veetil, B. D. Nelson, R. E. Guldberg, and K. G. Ong, "An embedded wireless temperature sensor for orthopedic implants," *IEEE Sensors Journal*, vol. 18, no. 3, pp. 1265–1272, 2017.

[12] L. Balocchi, V. Palazzi, S. Bonafoni, F. Alimenti, P. Mezzanotte, and L. Roselli, "Wireless passive temperature sensor based on a harmonic transponder and a thermistor," in *2023 IEEE 13th International Conference on RFID Technology and Applications (RFID-TA)*, IEEE, 2023, pp. 150–153.

[13] W. Qian and C. Qian, "Long-range detection of a wirelessly powered resistive transducer," *IEEE Transactions on Instrumentation and Measurement*, vol. 71, pp. 1–9, 2022.

[14] A. Albrecht, J. F. Salmeron, M. Becherer, P. Lugli, and A. Rivadeneyra, "Screen-printed chipless wireless temperature sensor," *IEEE Sensors Journal*, vol. 19, no. 24, pp. 12 011–12 015, 2019.

[15] S. U. Amin, M. A. Shahbaz, S. A. Jawed, *et al.*, "A wirelessly powered low-power digital temperature sensor," *International Journal of Circuit Theory and Applications*, vol. 48, no. 4, pp. 485–501, 2020.

[16] International Committee for Animal Recording (ICAR), "International Agreement of Recording Practices," pp. 433–434, Jun. 2008.

[17] A. Seré, L. Steinfeld, S. Hemour, and P. Pérez-Nicoli, "Self-adaptive intermediate resonator in a 3-coil inductive link for power and data transmission," *IEEE Transactions on Circuits and Systems II: Express Briefs*, 2024.

[18] S. P. Gentile, "Basic theory and application of tunnel diodes," *(No Title)*, 1962.

[19] E. G. R. W. H. R. Lowry J. Giorgis, *Tunnel Diode Manual*. General Electric, 1961.

[20] P. Pérez-Nicoli, M. Sivolella, N. Gammarano, and F. Silveira, "Limits for increasing the WPT distance in AIMDs," in *2020 XXXIIIrd General Assembly and Scientific Symposium of the International Union of Radio Science*, IEEE, 2020, pp. 1–4.